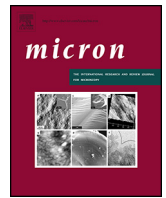




Contents lists available at ScienceDirect

Micron

journal homepage: www.elsevier.com/locate/micron

Estimation of martensite feature size in a low-carbon alloy steel by microtexture analysis of boundaries

T. Karthikeyan*, Manmath Kumar Dash, S. Saroja, M. Vijayalakshmi

Physical Metallurgy Group, Metallurgy and Materials Group, Indira Gandhi Centre for Atomic Research, Kalpakkam 603102, India

ARTICLE INFO

Article history:

Received 16 July 2014

Received in revised form

26 September 2014

Accepted 26 September 2014

Available online xxx

Keywords:

Steels

Orientation relationship

Martensite boundaries

Microtexture analysis

EBSD

ABSTRACT

A methodology for classifying the hierarchy of martensite boundaries from the EBSD microtexture data of low-carbon steel is presented. Quaternion algebra has been used to calculate the ideal misorientation between product α variants for Kurdjumov–Sachs (KS) and its nearby orientation relationships, and arrive at the misorientation angle-axis set corresponding to packet (12 types), block (3 types) and sub-block boundaries. Analysis of proximity of experimental misorientation between data points from the theoretical misorientation set is found to be useful for identifying the different types of martensite boundaries. The optimal OR in the alloy system and the critical deviation threshold for identification of martensite boundaries could both be ascertained by invoking the ‘Enhancement Factor’ concept. The prior- γ grain boundaries, packet, block and sub-block boundaries could be identified reasonably well, and their average intercept lengths in a typical tempered martensite microstructure of 9Cr–1Mo–0.1C steel was estimated as 31 μm , 14 μm , 9 μm and 4 μm respectively.

© 2014 Published by Elsevier Ltd.

1. Introduction

Quantitative assessment of materials microstructure is needed to study its influence on functional properties, and to optimize the desirable structure for various applications. The (tempered) martensite microstructure in steels exhibits a complex morphology with a high density of boundaries and defects, and the interface separating the tiny ferrite crystallites of bcc- α /bcc- α' are not well delineated in optical or scanning electron microscopy (SEM) micrographs. The prior-austenite (γ) grain size (PAGS) is an important microstructural parameter influencing the steel property, and specific etchants (such as Vilella's reagent or thermal etching) are used to bring out the prior- γ grain boundaries for measurement (García de Andres et al., 2003). In addition, the martensite packet, block and lath sizes regulate the mechanical properties of low-carbon steels (Nagasaka et al., 2000; Morito et al., 2006; Wang et al., 2008; Luo et al., 2010; Zhang et al., 2012). Recently, the SEM-Electron Backscatter Diffraction (EBSD) technique has been utilized to characterize the microtexture in bainitic/martensitic steels, and study the distribution of product α crystallites within prior- γ grains (Gourgues et al., 2000; Morito et al., 2003; Kitahara et al., 2006; Stormvinter et al., 2012; Takayama et al., 2012). Orientation relationship (OR) is known to operate between γ/α crystals

in martensitic transformation, and the product α variants are then inter-related by specific misorientations, expressed through misorientation angle-axis set (Sonderegger et al., 2007; Zachrisson et al., 2013; Karthikeyan et al., 2013; Beladi et al., 2014; Cayron, 2014). Based on EBSD studies, the general hierarchy of lath martensitic structure and a scheme to identify boundaries outlining the packet, block and sub-block features in low-carbon steel has been formulated by applying Kurdjumov–Sachs (KS) OR (Morito et al., 2003; Kitahara et al., 2006). In the KS relation $\{111\}\gamma//\{110\}\alpha$ $\langle 110\rangle\gamma//\langle 111\rangle\alpha$, the choice for γ governing plane (4 types) and the γ governing direction within the plane (6 types) give rise to 24 possible product variants. The set of six variants with the same γ governing plane tend to form together as packets with a common habit plane. The six variants within each packet are distributed as parallel blocks (of up to 3 types), with each block consisting of a pair of variants separated by a sub-block boundary of small misorientation angle. Analysis of neighboring α crystallite domains in microtexture maps based on expected misorientation across sub-block/block/packet boundaries (supported with band contrast/image quality images) has been used to identify and measure martensite features in low-carbon steels (Wang et al., 2008; Zhang et al., 2012). The present study reports the development of a generalized routine for automated classification of martensite boundaries from EBSD data, and demonstrates the estimation of average size of prior- γ grain, packet, block and sub-block features in a tempered martensite microstructure of 9Cr–1Mo–0.1C (mass %) steel.

* Corresponding author. Tel.: +91 44 27480306.

E-mail address: tkarthi@igcar.gov.in (T. Karthikeyan).

The KS and Nishiyama–Wassermann (NW) $\{111\}\gamma//\{110\}\alpha$ ($112\}\gamma//\{110\}\alpha$) relations based on parallelism of simple planes/directions are often used for interpretation of OR in steels. However, the exact governing OR could differ depending on the steel composition and phase transformation temperature, and also exhibit scatter from the average OR (Kelly et al., 1990; Miyamoto et al., 2009; Germain et al., 2012; Stormvinter et al., 2012). Based on Transmission Electron Microscopy (TEM) Kikuchi line pattern analysis in a low-carbon low-alloy steel, the orientation relation between martensite lath and retained austenite has been deduced by Kelly et al. (1990) as: $\{111\}\gamma$ nearly parallel to $\{110\}\alpha$, $(110)\gamma$ 1.5–3° away from $(111)\alpha$. The Kelly OR is similar to the Greninger–Troiano (GT) OR originally observed in iron–nickel–manganese alloy stated as: $(111)\gamma \sim (011)\alpha'$, $[\bar{1}01]\gamma \sim [\bar{1}\bar{1}1]\alpha'$ (Nishiyama, 1978). The Kelly and GT relations could be considered to be approximately in-between KS–NW OR, with an average deviation (from KS) of 1.5–3° and 2.5° respectively. Analysis of OR by TEM have limited statistics, and recently, several EBSD based methods have been proposed for a rigorous determination of average OR. These methods rely on segregation of microtexture data from a single prior- γ grain and determination of optimum OR by suitable data analysis. Based on numerical fitting procedure that minimizes the average misorientation, the average OR in a low-carbon martensite steel has been deduced; the close packed planes of $\{111\}\gamma$ and $\{110\}\alpha$ are found to be away by about 1.7°, unlike the KS, NW and Kelly relations (Miyamoto et al., 2009). Comparison of high index pole figure distribution of α between experiment and that calculated from γ grain orientation and OR has been sought to improve the accuracy of detected OR (Nolze, 2006). The best representative OR in a low-carbon steel with a tempered martensite structure has been solved using quaternions and optimization theory, and the deduced OR was found to differ from KS and NW relations by 3.8° and 2.6° respectively (Humbert et al., 2011). Recently, EBSD pole figure results have been used to interpret the OR of bainitic and high Cr martensitic steels (with low-C/high-C contents) using the phenomenological theory of martensite crystallography (PTMC) (Chintha et al., 2013). Based on the distribution of rotation axis in small angle and large angle grain boundaries in tempered martensite structure of 9–12% Cr steel, a mixed model of KS/NW had been proposed (Sonderegger et al., 2007). Boundaries in tempered martensite structure of Fe–Cr alloy have been analyzed based on misorientation angle distribution, and image quality maps at higher resolution was used to reveal the distribution of carbides along small and large angle boundaries (Tak et al., 2009). Recently, representation of boundary misorientations in Rodrigues–Frank space and experimentally determined OR were utilized to distinguish intra- and inter-packet boundaries and determine their amounts (Zachrisson et al., 2013). In some studies, morphology of the grain boundary segment have been additionally assessed to confirm the closeness of habit plane to $\{111\}\gamma//\{110\}\alpha$ [Morito et al., 2006]. In order to develop an optimum procedure for classification of martensite boundaries, it is important to know the representative OR in the alloy system and the extent of scatter from ideal misorientations. The methodology contrived in the present work can predict the average OR from large EBSD dataset and help to choose suitable tolerance settings for classification of boundaries.

2. Experimental

The 9Cr–1Mo–0.1C steel (Grade P9) after normalizing (1323 K/1 h/air cooling) and tempering (1023 K/2 h/air cool) treatment was investigated in a W-filament XL 30 SEM (FEI) equipped with a Channel 5 EBSD system (Oxford/HKL) (Karthikeyan et al.,

2013). A relatively low magnification was chosen so as to cover a large number of austenite grains, and dynamic focusing was actuated to achieve a uniform focus across the 70° tilted specimen. A large area scan (2000 × 712 pixels with 0.6 μm step size) of ~12 h duration was conducted, and overall indexing rate was 73%. This scan data was extensively investigated by microtexture analysis (elaborated in Section 4.2). The scan data was also processed using the EBSD software, and standard subroutines were used to remove isolated erroneous data points and to assign orientation to non-indexed points based on its surrounding points. The processed microtexture dataset was analyzed to generate various martensite boundary maps and obtain estimate of martensite feature size (Section 4.3). Additionally, a high resolution EBSD scan (with smaller probe size ~0.1 μm , 0.2 μm step size) was conducted to improve data quality (to 86% indexing), and the martensite boundary distribution was assessed.

3. Misorientation relation of martensite boundaries

In literature, the matrix methods have been used for stating the OR equation, and to find the misorientations between variants (Kitahara et al., 2006; Sonderegger et al., 2007; Abbasi et al., 2012; Jonas et al., 2014). Though less popularly used, the mathematical quantity of Quaternions are well suited for describing rotation operations, and orientation calculations could be adeptly performed using quaternion algebra (Altmann, 1989; Morawiec, 2003). A rotation process can be mathematically described by a unit quaternion,

$$\begin{aligned} \mathbf{q}(\theta, \hat{\mathbf{n}}) &= \mathbf{q}(\theta, n_1\hat{\mathbf{i}} + n_2\hat{\mathbf{j}} + n_3\hat{\mathbf{k}}) \\ &= \cos\left(\frac{\theta}{2}\right) + \sin\left(\frac{\theta}{2}\right) [n_1\hat{\mathbf{i}} + n_2\hat{\mathbf{j}} + n_3\hat{\mathbf{k}}] \end{aligned} \quad (1)$$

where θ is the rotation angle, and $\hat{\mathbf{n}}$ is the axis of rotation. The quaternion equation relating the orientation of product α with the orientation of parent γ can be stated as,

$$\mathbf{q}\alpha = \mathbf{q}\gamma \cdot \mathbf{q}\text{OR} \quad (2)$$

where $\mathbf{q}\alpha$, $\mathbf{q}\gamma$ are unit quaternions denoting the orientation of α , γ crystals with respect to the reference coordinate axis, and the $\mathbf{q}\text{OR}$ unit quaternion denotes the relative rotation required to align the governing planes and directions of the two crystals.

3.1. Ideal Kurdjumov–Sachs relation

If the specific instance of KS relation between a reference ferrite variant α_0 and a parent γ crystal is taken as $(1\bar{1}1)\gamma//(\bar{0}\bar{1}1)\alpha_0$, $[\bar{1}01]\gamma//[\bar{1}\bar{1}1]\alpha_0$ then,

$$\mathbf{q}\alpha_0 = \mathbf{q}\gamma \cdot \mathbf{q}\text{KS} = \mathbf{q}\gamma \cdot \mathbf{q}(42.85^\circ, [0.1776 \ 0.1776 \ 0.9679]) \quad (3)$$

where the relative rotation between α_0/γ crystals is specified through the minimum rotation angle, rotation axis components (He et al., 2005). A geometrical method for the derivation of rotation axis and angle of the $\mathbf{q}\text{KS}$ is given in Appendix A. Using the procedure described in Appendix B, the misorientation between product ferrite variants have been calculated. The resultant types of misorientation angle and rotation axis vectors (of unit magnitude) between pair of variants are given in Table 1, and the scheme given by Morito et al. (2003) has been adopted to classify the boundary separating such variants as sub-block, block and packet boundaries (SBB, BB and PB).

The different types of BB and PB are 3 and 12 respectively, and they have been labeled sequentially in ascending order of misorientation angle. The family of $\langle r_1 r_2 r_3 \rangle$ – rotation axis and $\pm\omega$ – rotation angle have been considered to count all distinct symmetries, and

Download English Version:

<https://daneshyari.com/en/article/7986723>

Download Persian Version:

<https://daneshyari.com/article/7986723>

[Daneshyari.com](https://daneshyari.com)